



Technical Note

Suppression of Marangoni convection of silicon melt by a non-contaminating method

Jie Li ^a, Mingwei Li ^{a,*}, Wenrui Hu ^b, Danling Zeng ^a^a Institute of Power Engineering, Chongqing University, Chongqing 400044, China^b Institute of Mechanics, CAS, Beijing 100083, China

Received 23 January 2003; received in revised form 5 June 2003

Abstract

A set of numerical simulation of the effect of the gas shearing flow over a silicon melt free surface on Marangoni convection under microgravity condition was conducted by using finite element method. For given gas channel width, Marangoni number and aspect ratio a remarkable reduction of Marangoni convection in silicon liquid bridge can be achieved by choosing the optimal gas velocity in accordance with the correlation proposed in the paper. The effectiveness of the reduction of the gas flow under different conditions shows that, in some cases, Marangoni convection reduction of 99% can be realized by this non-contaminating method.

© 2003 Elsevier Ltd. All rights reserved.

Keywords: Marangoni convection; Silicon; Non-contamination method; Finite-element method

1. Introduction

It is well known that Marangoni convection (MC) dominating under microgravity gives strong influence on the crystal growth process. Space experiments conducted by Eyer et al. [1] have shown that time-dependent MC will lead to solute segregation which is the underlying cause of striation. The floating-zone method by the combination with microgravity environment is expected a promising containerless method for the growth of striation-free crystal, but the MC must be suppressed effectively. In order to produce high-quality semiconductor, some approaches such as liquid encapsulant method, have been applied to reduce the Marangoni convection [2–10]. Besides, a non-contaminating method [11] to reduce MC was suggested and investigated experimentally by Dressler et al., where a vertical jet of gas (argon) was blown tangentially over the free surface, producing a viscous shearing drag opposing the thermocapillary shear at the surface. A small drop of silicone oil with 1.5 mm

height was chosen, which was confined in a transparent box (1.5 mm × 1.5 mm × 2.5 mm) with one vertical side open for the free surface. Their experimental results show that the MC velocity reduction of 66% can be achieved. In the global simulation of a silicon Czochralski furnace, it was found that the gas flow has a significant influence on the melt convective pattern [12]. However, up to now, there is no investigation report associated with applying this method to suppress the MC in silicon liquid bridge to our knowledge.

In the present work, a set of numerical simulation to investigate the effect of argon gas viscous shearing flow on MC in silicon liquid bridge is performed under different gas channel width, Marangoni number and aspect ratio of the height to radius by finite element method. The results show that a significant reduction of Marangoni convection in the silicon melt can be realized.

2. Model formulation

2.1. Physical model

Consider an axisymmetric silicon melt column contained between two planar disks with a height H apart,

* Corresponding author. Tel.: +86-23-654-15008; fax: +86-23-651-02473/02471.

E-mail address: mwlizao@yahoo.com (M. Li).

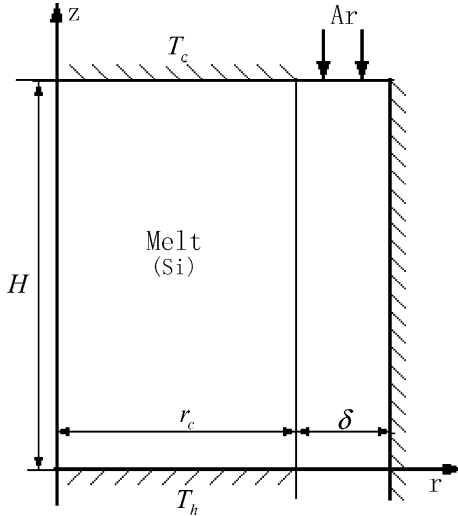


Fig. 1. Physical model.

as shown in Fig. 1. Argon gas flows surrounding the free surface from the cold end to the hot end. Let r_c be the radius of the melt, δ be the width of the channel. The silicon melt is assumed to be incompressible Newtonian fluid; and the liquid–gas interface is smooth and non-deformable. The endwalls at $z = 0, H$ are maintained at constant temperature T_h and T_c , respectively. The law of surface tension versus temperature is assumed to be linear:

$$\sigma = \sigma_c - \gamma(T - T_c), \quad (1)$$

in which σ_c is the surface tension of the melt–gas interface at temperature T_c ($T_c = T_m = 1683$ K), γ is the variation rate of surface tension with temperature T , $\gamma = -\partial\sigma/\partial T$. Gravity is assumed to be absent.

2.2. Mathematical model

2.2.1. Governing equations

In the governing equation, the dimensionless parameters (with asterisks) are adopted which are defined as follows:

$$\begin{aligned} r &= r_c r^*, & z &= z^* H, & \delta &= r_c \delta^* & u_i &= u_i^* \frac{v_1}{r_c}, \\ v_i &= v_i^* \frac{v_1}{r_c}, & p_i &= \frac{\rho_1 v_1^2}{r_c^2} p_i^*, & T_i &= (T_h - T_c) T_i^* + T_c, \\ \rho_i &= \rho_i^* \rho_1, & \lambda_i &= \lambda_i \lambda_1^*, & \mu_i &= \mu_i^* \mu_1, & \kappa_i &= \kappa_i^* \kappa_1, \end{aligned}$$

where r and z are the radial and the axial coordinate, respectively, u_i is the radial velocity components and v_i the axial velocity components, p_i the pressure, T_i the temperature, ρ_i the density, λ_i the thermal conductivity, v_1 the kinematic viscosity of melt, μ_i the dynamic viscosity and κ_i the thermal diffusivity, respectively.

Subscripts i indicate Silicon melt ($i = 1$), Argon gas ($i = g$), respectively.

The dimensionless general governing equations of momentum and energy are given as follow with the asterisk dropped conventionally:

$$\frac{1}{r} \cdot \frac{\partial(r u_i)}{\partial r} + \frac{1}{A} \frac{\partial v_i}{\partial z} = 0, \quad (2)$$

$$\begin{aligned} \rho_i \left(u_i \frac{\partial u_i}{\partial r} + \frac{1}{A} v_i \frac{\partial u_i}{\partial z} \right) &= - \frac{\partial p_i}{\partial r} + \mu_i \left(\frac{\partial^2 u_i}{\partial r^2} + \frac{1}{A^2} \frac{\partial^2 u_i}{\partial z^2} \right. \\ &\quad \left. + \frac{1}{r} \frac{\partial u_i}{\partial r} - \frac{u_i}{r^2} \right), \end{aligned} \quad (3)$$

$$\begin{aligned} \rho_i \left(u_i \frac{\partial v_i}{\partial r} + \frac{1}{A} v_i \frac{\partial v_i}{\partial z} \right) &= - \frac{1}{A} \frac{\partial p_i}{\partial z} + \mu_i \left(\frac{\partial^2 v_i}{\partial r^2} + \frac{1}{A^2} \frac{\partial^2 v_i}{\partial z^2} + \frac{1}{r} \frac{\partial v_i}{\partial r} \right), \end{aligned} \quad (4)$$

$$Pr_i \left(u_i \frac{\partial T_i}{\partial r} + \frac{1}{A} v_i \frac{\partial T_i}{\partial z} \right) = \kappa_i \left(\frac{\partial^2 T_i}{\partial r^2} + \frac{1}{r} \frac{\partial T_i}{\partial r} + \frac{1}{A^2} \frac{\partial^2 T_i}{\partial z^2} \right), \quad (5)$$

where Prandtl number is defined by $Pr_i = \rho_i c_{pl} v_1 / \lambda_i$, c_{pl} the specific heat of melt, and A the aspect ratio $A = H/r_c$.

2.2.2. Boundary conditions

At the cold endwall of the melt:

$$u_i = v_i = 0, \quad T_i = 0. \quad (6a-c)$$

At the inlet of the gas channel:

$$u_g = 0, \quad v_g = v_{in}, \quad T_g = 0. \quad (6d-f)$$

At the hot endwall of the melt:

$$u_i = v_i = 0, \quad T_i = 1. \quad (6g-i)$$

At the side wall of the gas channel:

$$u_g = v_g = 0, \quad T_g = T(z). \quad (6j-l)$$

At the melt/gas interface:

$$u_i = 0, \quad u_g = 0, \quad v_i = v_g, \quad (6m-o)$$

$$T_i = T_g, \quad (6p)$$

$$-\lambda_i \frac{\partial T_i}{\partial r} = -\lambda_g \frac{\partial T_g}{\partial r}, \quad (6q)$$

$$\frac{\partial u_i}{\partial r} - \mu_g \frac{\partial u_g}{\partial r} = -Ma \cdot \frac{1}{A} \frac{\partial T}{\partial z}, \quad (6r)$$

where v_{in} is the dimensionless inlet gas velocity (hereafter this is called gas velocity for short). The dimensionless Marangoni number Ma in equation is defined as follows:

$$Ma = \frac{\Delta T \cdot r_c \gamma}{\mu_1 v_1},$$

here $\Delta T = T_h - T_c$.

The numerical procedure used here and the related physical properties needed in the calculation can be found in Ref. [12].

3. Results

A set of numerical simulation of flow and heat transfer in both melt and gas phases for different gas velocity in the case of $\delta = 0.3$, $A = 2.0$ and $Ma = 108,000$ was conducted. The suppressive effect of gas flow on the melt convection was observed from the results obtained. Because of the length limit of the paper, only two figures of the contours of stream function and isothermals of the silicon melt and the gas with two different gas velocity are presented in Figs. 2 and 3, respectively. It should be emphasized that the low gas velocity gives a little influence on MC, a large counter clockwise Marangoni convection vortices still occupy the bulk melt. The highest velocity of the melt occurs at

the melt/gas interface. The distorted isothermal depicted that convection heat transfer is dominated in the melt. In this case, due to the continuity conditions must be satisfied at the melt/gas interface, the strong Marangoni convection results in an upward flow of gas phase in the adjacent of the melt/gas interface. With gradually increasing gas velocity, the induced upward gas flow slows down and eventually dies away. Inversely, viscous shearing drag of gas acting on the melt surface makes Marangoni convection become weaker and weaker, as the gas velocity goes to a certain value, in the present case, when $v_{in} = 24,300$, i.e. 67.23 cm/s, the dimensionless average velocity of the melt $v_{av,g}$ reaches the minimum value, i.e. $v_{av,g} = 30.64$, 0.085 cm/s. Here $v_{av,g}$ stands for the non-dimensional average velocity of the melt defined by $v_{av,g} = \sum(\sqrt{u_i^2 + v_i^2})/N$, in which N represents the total number of the nodes in the region of the melt. After the minimum value has reached, the dimensionless average velocity increases again and the melt flow pattern tends to be more complicated. Therefore, we can conclude that there exists an extreme value of the non-dimensional average velocity of the melt which reflects the weakest flow of the melt. Undoubtedly, an effective suppression can be achieved by properly choosing the gas velocity for a specified condition.

To quantitatively evaluate the effectiveness of flow reduction caused by gas flow on the melt convection for different gas channel width δ , Marangoni number Ma and aspect ratio A , a parameter PR called reduction percentage was introduced:

$$PR = \frac{-(v_{av,g} - v_{av})}{v_{av}} \times 100\%$$

where v_{av} denotes the non-dimensional average velocity of the melt without gas flow. Fig. 4 indicates the change of the non-dimensional average velocity of the melt $v_{av,g}$

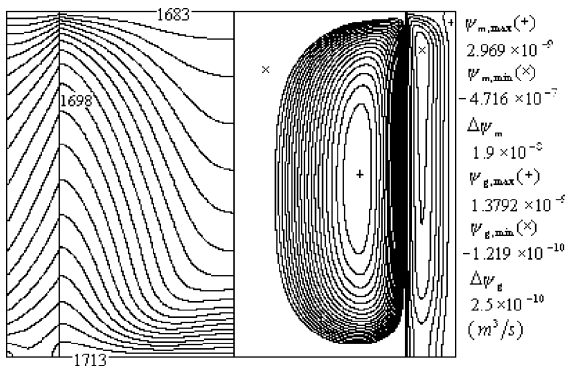


Fig. 2. Isotherms (left, $\Delta T = 1.5$ K) and contours of stream function of melt and gas (right) with $A = 2.0$, $\delta = 0.3$, $Ma = 1.08 \times 10^5$, $v_{in} = 500$.

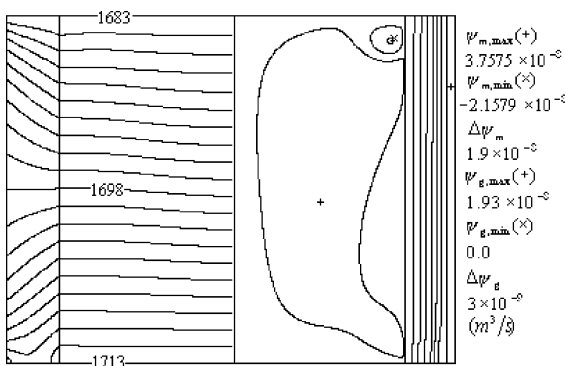


Fig. 3. Isotherms (left, $\Delta T = 1.5$ K) and contours of stream function of melt and gas (right) with $A = 2.0$, $\delta = 0.3$, $Ma = 1.08 \times 10^5$, $v_{in} = 24,300$.

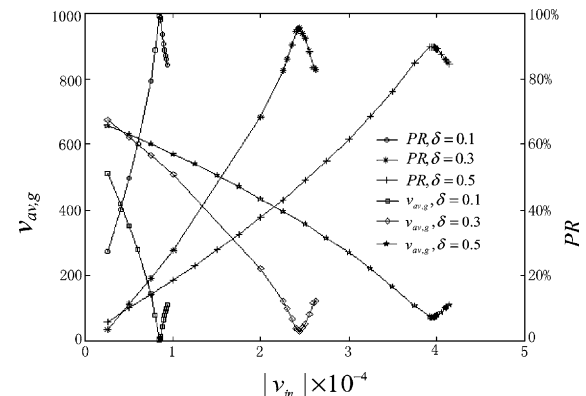


Fig. 4. Average velocity $v_{av,g}$ and reduction percentage PR versus gas velocity v_{in} for various gas channel width δ with $A = 2.0$, $Ma = 1.08 \times 10^5$.

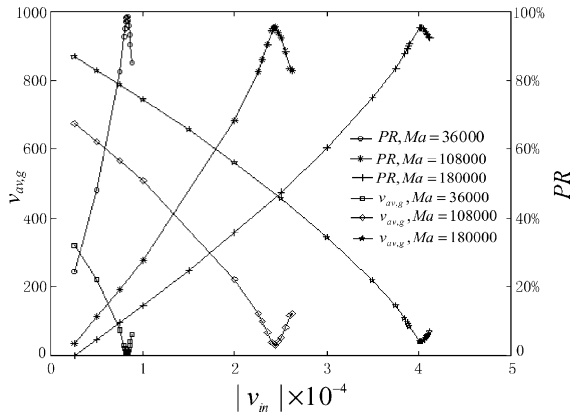


Fig. 5. Average velocity $v_{av,g}$ and reduction percentage PR versus gas velocity v_{in} for various Marangoni number Ma with $A = 2.0$, $\delta = 0.3$.

and reduction percentage PR with the gas velocity v_{in} for various gas channel width δ . The values of v_{in} and PR corresponding to extreme points of the curves PR– v_{in} are nothing but the optimal gas velocity ($v_{in,opt}$) and reductive effectiveness (PR_b), respectively. The value of $v_{in,opt}$ decreases from 39,500 (109.3 cm/s) to 8450 (23.34 cm/s) and the value of PR_b increases from 89.82% to 99.47% when reducing the value of δ from 0.5 to 0.1, this means that narrowing the width of the gas channel is beneficial for suppressing Marangoni convection. This is consistent qualitatively with the result of Ref. [8].

In the situation of the fixed gas channel width and aspect ratio, a higher optimal gas velocity $v_{in,opt}$ is required, meanwhile the value of PR_b has a slightly decrease with increasing Marangoni number Ma (see Fig. 5).

For different aspect ratio A , the values of $v_{in,opt}$ and PR_b are different, as shown in Fig. 6. The change of the

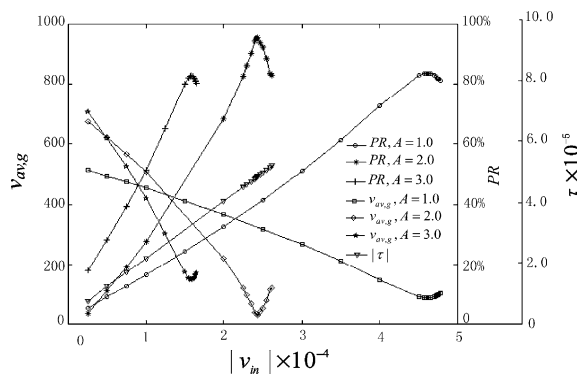


Fig. 6. Average velocity $v_{av,g}$, reduction percentage PR and shearing stress τ versus gas velocity v_{in} for various aspect ratio A with $\delta = 0.3$, $Ma = 1.08 \times 10^5$.

PR_b and $v_{in,opt}$ with A is not monotonous. When $A = 2.0$, the value of PR_b becomes the highest, $PR_b = 95.62\%$. Meanwhile one can find that the shearing stress acting on the silicon surface increases linearly as the gas velocity increases for the fixed values of δ , A and Ma .

From the numerical result obtained, the optimal gas velocity can be expressed in the following correlation:

$$v_{opt} = 1.762 \cdot \delta^{0.9562} \cdot A^{-0.9655} \cdot Ma^{0.9788} \quad (7)$$

with the correlative coefficient of 0.99. This correlation provides us an approximate choice of the gas velocity so that the highest degree of reduction of Marangoni convection can be realized.

4. Conclusions

A non-contaminating method for suppressing Marangoni convection in a silicon liquid bridge was realized by introducing a tangential flow of Argon gas passing over the silicon melt free surface, thus to form a viscous shear drag opposing to Marangoni shearing at the free surface. Numerical simulation using finite element method was conducted to demonstrate the effectiveness of the approach. The effectiveness of the reduction of the flow is associated with the inlet gas velocity for given conditions. By properly choosing the gas velocity, the optimal reductive effectiveness of Marangoni convection can be achieved. The optimal reductive effectiveness under different gas channel width, Marangoni number and aspect ratio has been presented. It is proved that the MC reduction of 99% can be realized in some situation.

Acknowledgements

This work was supported by the Excellent Young Teachers Program of MOE (EYTP), P.R.C. [2002] 40 and by National Microgravity Laboratory, Institute of Mechanics, Chinese Academy of Science.

References

- [1] A. Eyer, H. Leiste, R. Nitsche, Float zone growth of silicon under microgravity in a sounding rocket, *J. Cryst. Growth* 71 (1985) 173–182.
- [2] A. Eyer, H. Leiste, Striation-free silicon crystal by float-zoning with surface-coated melt, *J. Cryst. Growth* 71 (1985) 249–252.
- [3] T. Doi, J. Koster, Marangoni convection in two immiscible liquid layers subject to a horizontal temperature gradient, in: *Proceedings of the 7th International Conference on Physico-chemical Hydrodynamics*, MIT, Cambridge, MA, 1989.

- [4] E. Crespo del Arco, G.P. Extremet, R.I. Sani, Thermocapillary convection in a two-layer fluid system with flat interface, *Adv. Space Res.* 11 (1991) 129–132.
- [5] J. Li, J. Sun, Z. Saghir, Buoyant and thermocapillary flow in liquid encapsulated float zone, *J. Cryst. Growth* 131 (1993) 83–96.
- [6] Q.S. Liu, G. Chen, B. Roux, Thermogravitational and thermocapillary convection in a cavity containing two superposed immiscible liquid layers, *Int. J. Heat Mass Transfer* 36 (1993) 101–117.
- [7] J. Li, M.Z. Saghir, Thermocapillary convection in liquid encapsulation float zone, in: *Int. Symp. On Microgravity Science and Application*, Beijing, China, 1993.
- [8] M. Li, D. Zeng, The effect of liquid encapsulation on the Marangoni convection in a liquid column under microgravity condition, *Int. J. Heat Mass Transfer* 39 (17) (1996) 3725–3732.
- [9] Q.S. Liu, B. Roux, M.G. Velarde, Thermocapillary convection in two-layer systems, *Int. J. Heat Mass Transfer* 41 (11) (1998) 1499–1511.
- [10] M. Li, D. Zeng, T. Zhu, Instability of the Marangoni convection in a liquid bridge with liquid encapsulation under microgravity condition, *Int. J. Heat Mass Transfer* 45 (2002) 157–164.
- [11] R.F. Dressler, N.S. Sivakumaran, Non-contaminating method to reduce Marangoni convection in microgravity float-zones, *J. Cryst. Growth* 88 (1988) 148–158.
- [12] M. Li, Y. Li, N. Imaishi, T. Tsukada, Global simulation of a silicon Czochralski furnace, *J. Cryst. Growth* 234 (2002) 32–46.